THE JOURNAL OF PHYSICAL CHEMISTRY C

Article

Cite This: J. Phys. Chem. C 2020, 124, 1469−1477

pubs.acs.org/JPCC

A Model Protometabolic Pathway across Protocell Membranes Assisted by Photocatalytic Minerals

Punam Dalai[†] and Nita Sahai*[,†,‡,§]

[†]Department of Polymer Science, University of Akron, 170 University Avenue, Akron, Ohio 44325, United States

[‡]Department of Geosciences, University of Akron, Akron, Ohio 44325, United States

[§]Integrated Bioscience Program, University of Akron, Akron, Ohio 44325, United States

Supporting Information

ABSTRACT: Protocell analogs (lipid vesicles) to modern cell membranes have been postulated as compartments that may have been involved in primordial metabolism during the transition from geochemistry to biochemistry on early Earth. The transduction of light energy into chemical energy for metabolism was a key step in the transition from the earliest metabolisms to phototrophy. Photocatalytic minerals may have served the role of enzymes during these transitional stages. Here, we demonstrate a simple photoheterotrophic protometabolism promoted by photocatalytic minerals across a model protocell (vesicle) membrane. These minerals in the extra-vesicular medium utilized light energy to drive a coupled, multistep transmembrane electron transfer reaction (TMETR), while simultaneously generating a transmembrane pH gradient and reducing nicotinamide adenine dinucleotide (NAD^+) to NADH within the vesicle. The proton gradient or chemiosmotic potential could have provided a basis for adenosine triphosphate (ATP) synthesis and NADH could potentially have driven further metabolic chemistry inside the protocells.

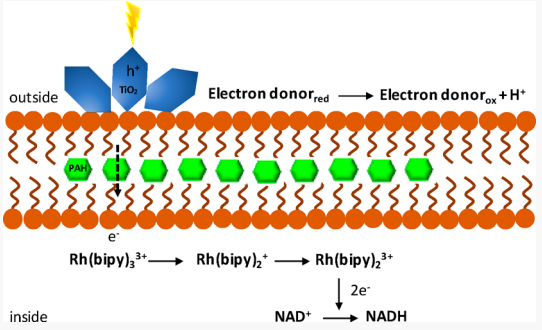

1. INTRODUCTION

The origin of protometabolism before enzymes existed is one of the central issues in origins of life studies. Modern metabolic processes are multistep, coupled redox reaction cycles that are catalyzed by specific enzymes. These enzymes are assisted by cofactors such as NAD^+ and nicotinamide adenine dinucleotide phosphate ($NADP^+$) and their reduced forms NADH and NADPH, respectively. In most metabolisms, the reduction of $NAD(P)^+$ to NAD(P)H is linked to the generation of a transmembrane pH gradient or chemiosmotic potential, which drives ATP synthesis. The importance of a transmembrane pH gradient in developing protometabolism has been highlighted.[1−3] Furthermore, recognizing the metabolic significance of NAD even in an "RNA world" scenario, a prebiotic synthesis of NAD has been achieved recently.[4]

A cell membrane defines the cell by providing a boundary separating the inner components from the environment. It has been proposed that self-assembling vesicles of single chain amphiphiles (SCAs) could have served as compartments for performing the first metabolism on the prebiotic Earth.[5] These SCA vesicles have been widely studied as model protocells due to their prebiotic availability, their similarity to modern phospholipid membranes in their ability for growth, division and encapsulating water-soluble solutes to catalyze reactions as reviewed recently.[6−9] Thus, lipid membrane protocells have the advantage of being able to grow and divide, which distinguishes them from other model protocell systems such as "mineral membranes" and coacervates. Mixed fatty acid and phospholipid membranes have also been studied[10−13] and found to possess enhanced stability toward metal ions that are ubiquitous in most geochemical environments.[12,13]

It has been hypothesized by some that the first cells may have evolved chemoautotrophic metabolisms at oceanic hydrothermal vents[1,2] whereas others have argued for heterotrophy.[14,15] An ideal model (proto)cell metabolism system should at least be able to both generate a transmembrane pH gradient by a transmembrane electron transfer reaction (TMETR) as well as drive an intracellular coupled redox reaction cycle. Various attempts have been made to mimic parts of protometabolism nonenzymatically in model protocells[16−18] as well as contemporary photoautotrophic metabolism in the absence or presence of enzymes for artificial light-harvesting systems.[19−21] In previous model (proto)cell systems, a one-step, TMETR was shown,[16,20,21] but these studies did not show a coupled reaction network inside the vesicle. In contrast, a two-step ETR with reductant, oxidant and photocatalytic mineral all enclosed within the vesicle was shown recently but this model system is not a transmembrane reaction.[18] Furthermore, a transmembrane pH gradient was not reported in any of these previous (proto)cell studies.[16−21] Progress has been made in establishing a proton gradient across precipitated iron sulfide mineral walls and by

Received: October 29, 2019
Revised: December 17, 2019
Published: December 23, 2019

DOI: 10.1021/acs.jpcc.9b10127
J. Phys. Chem. C 2020, 124, 1469−1477

thermophoresis in a water column but coupling to NAD^+ reduction was not shown in these cases.[22,23] Recently, the oxidation of NADH to NAD^+ and the generation of a reverse chemiosmotic potential across a membrane was shown using iron−sulfur cluster peptide complexes.[24] Here, we show that a model photoheterotrophic protometabolism could be developed in the presence of photocatalytic minerals as prebiotic enzymes to promote a multistep TMETR with simultaneous generation of a transmembrane pH gradient (chemiosmotic potential) and reduction of NAD^+ to NADH (Figure 1).

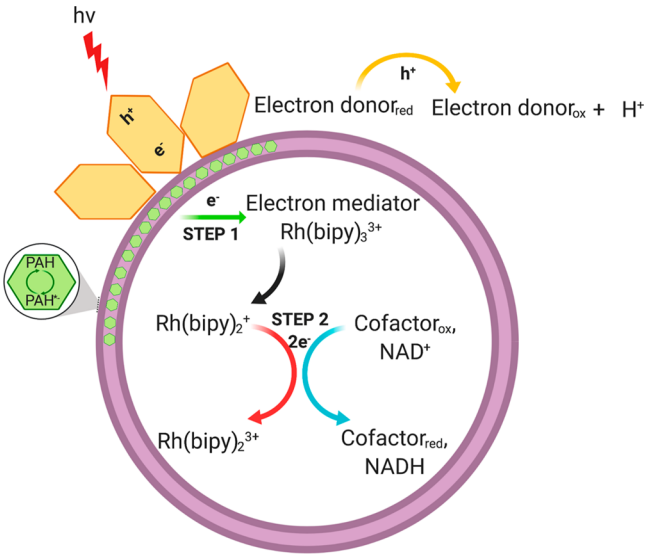

Figure 1. Schematic representation of coupled multistep TMETR network across a model protocell membrane in the presence of a photocatalytic mineral. The photocatalytic mineral acts as photosensitizer, the PAH is the electron shuttle and $Rh(bipy)_3^{3+}$ is the electron mediator. An extravesicular simple organic compound acts as terminal electron donor and NAD^+ represents the terminal electron acceptor. A representative TMETR system consists of lipid vesicles, 1-palmitoyl-2-oleoyl-glycero-3-phosphocholine (POPC) (2 mM) or oleic acid (OA) (7.5 mM); electron shuttle (50 μM, green hexagons), naphthopyrene (NP) or perylene; extravesicular photocatalytic mineral particles (0.5 mg/mL, yellow hexagons), TiO_2 or CdS or ZnO or FeS_2 or CdSe; electron donor (40 mM), serine or glycine or 2-propanol; $Rh(bipy)_3^{3+}$ complex (2.5 mM) and NAD^+ (15 mM) were present in the intravesicular medium.

The model protometabolism is composed of the following: (1) a lipid vesicle representing a model protocell; (2) an extravesicular reductant or sacrificial (terminal) electron donor (serine, glycine, 2-propanol); (3) photosensitizer or photocatalytic mineral; (4) an electron shuttle, a polyaromatic hydrocarbon (PAH), embedded within the membrane bilayer (either naphthopyrene or perylene); (5) an electron mediator, rhodium trisbipyridine ($Rh(bipy)_3^{3+}$) complex, encapsulated in the vesicle; and (6) a terminal electron acceptor, cofactor NAD^+, coencapsulated in the vesicle. The potential role of minerals in various aspects of the origins of life have long been postulated as reviewed elsewhere[25] but only recently have the mechanisms of mineral surface-promoted vesicle self-assembly and nonenzymatic RNA oligomerization been elucidated.[26,27] The present study is the first report showing that photocatalytic minerals such as, CdS, FeS_2, CdSe, TiO_2, and ZnO, present in the extra-vesicular medium can use light energy to drive transmembrane, coupled photoelectrochemical redox reactions inside vesicles, which produce a proton gradient and promote intravesicular reaction of reduction of NAD^+.

2. EXPERIMENTAL SECTION

Detailed experiment methodology is available in the Supporting Information.

2.1. General Procedure for Vesicle Preparation and Size Exclusion Chromatography. The 20 mM POPC and 75 mM OA vesicle solutions with 50 μM polyaromatic hydrocarbons (PAHs), 15 mM NAD^+ and 2.5 mM rhodium-(III)-tris(2,2′-bipyridine) trichloride ($Rh(bipy)_3Cl_3$) were prepared in bicine buffer (200 mM, pH 8.5) (Supporting Information). The vesicle samples were extruded 11 times through a 1 μm polycarbonate membrane to form monodisperse and single-bilayer vesicles (Figure S3). Afterward, vesicles encapsulated with NAD^+ and $Rh(bipy)_3Cl_3$ were separated from the unencapsulated solutes by gravity size-exclusion chromatography with a glass column filled with Sephadex G-50 medium beads. Fractions were collected by an automatic fraction collector and the absorbance was measured in a plate reader at 260 nm (NAD^+ absorbance peak) and 320 nm ($Rh(bipy)_3Cl_3$ absorbance peak) (Figure S3). Vesicle fractions containing encapsulated solutes were mixed together.

2.2. General Procedure of TMETR Experiments and NADH Enzymatic Assay. Mineral particles were characterized by transmission electron microscopy for approximate sizes (Figure S4 and Table S1). Photocatalytic mineral and terminal electron donor were added to the purified vesicle suspension (prepared as described in section 2.1 above), so that they were present in the extravesicular medium. The final mineral concentration was either 0.5 or 2.0 mg/mL and the terminal electron donor concentration was 40 mM. Subsequently, samples in septum-sealed glass vials were deoxygenated by purging with N_2 for 10 min. Afterward, sample vials were irradiated for 1, 2, and 3 h with UV lamp at 365 nm. Extraction of reaction products, removal of PAH from vesicles and removal of extra-vesicular minerals were achieved following the procedure from Summers and Rodoni[18] (Supporting Information). The emission spectrum of NADH was obtained by excitation at 340 nm and the NADH peak was detected at ∼450 nm. The confirmation for the formation of active NADH form was achieved by adding Na−pyruvate (25 mM) and the enzyme LDH (0.2 Units) to the extracted sample (Supporting Information). Prior to their addition, sample pH was adjusted to ∼7.5 using HCl.

2.3. Measurement of Proton Gradient Across Membrane. The 20 mM pure POPC or 75 mM OA vesicles encapsulated with 0.05 mM pyranine (8-hydroxypyrene-1,3,6-trisulfonic acid, HPTS) were prepared in buffer (200 mM bicine) to obtain the desired pH, between 7 and 9 (Supporting Information). The pH of buffer solutions was adjusted with sodium hydroxide. The vesicle samples were extruded through 1 μm pore of the polycarbonate membrane and were purified from unencapsulated dye by using size exclusion chromatography. Subsequently, sample vials were irradiated for 1, 2, and 3 h with UV lamp at 365 nm. Pyranine was excited at 402 and 460 nm, and emission was recorded at 510 nm. The ratio between these emissions (510/402 and 510/460 nm) depends on the change in the intravesicular pH. A calibration curve was made by using vesicles prepared at different pHs. For the TMETR experiment, CdS (0.5 mg/mL) was added to the vesicle suspension and samples were then exposed to UV radiation at 365 nm for 3 h. The change in the pyranine

DOI: 10.1021/acs.jpcc.9b10127
J. Phys. Chem. C 2020, 124, 1469−1477

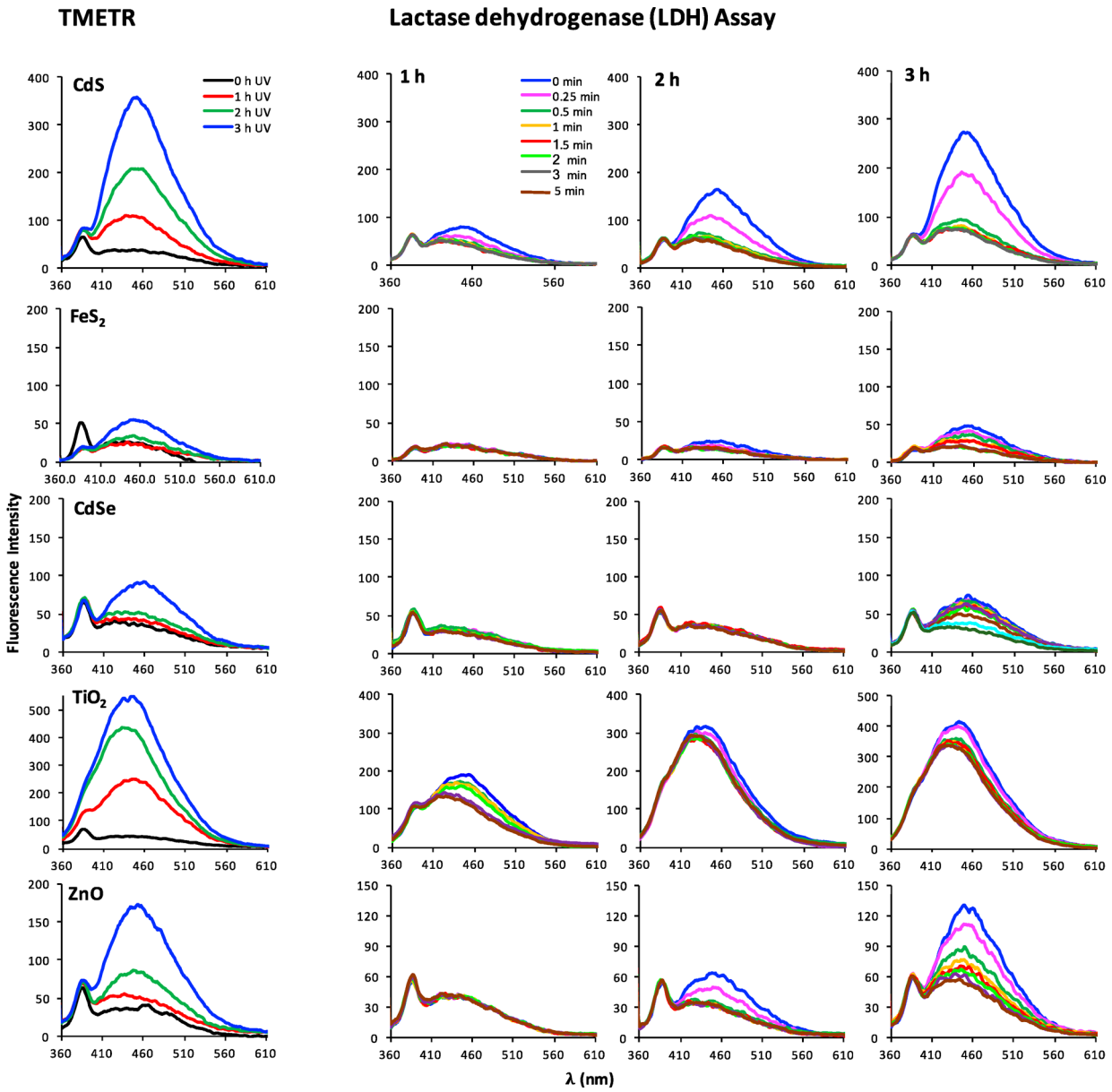

Figure 2. Coupled multistep TMETR photocatalyzed by various minerals using POPC vesicles and serine as the terminal electron donor. Emission spectra of NAD products generated after UV irradiation in the presence of various photocatalytic minerals. The system consists of POPC vesicles encapsulating NAD^+, extra-vesicular mineral and serine, and NP embedded in the bilayer. The first graph in each row (left panel) represents the total product formed after 0, 1, 2, and 3 h of UV irradiation and the remaining plots shows the LDH assay of the TMETR products at each time point (Supporting Information). The legends in the first graphs of both left and right panels are valid for the corresponding panels in the second to fourth rows. Experimental conditions: POPC (2 mM), naphthopyrene (50 μM), extravesicular mineral loading (0.5 mg/mL) and electron donor serine (40 mM), $Rh(bipy)_3^{3+}$ complex (2.5 mM), and NAD^+ (15 mM) in the intravesicular medium. See the Supporting Information for details.

fluorescence as a result of intravesicular pH change was measured every hour. All fluorescence measurements were performed by the plate reader (Synergy H1, BioTek Instruments, Winooski, VT).

2.4. Synthesis of Rhodium(III)–Tris(2,2′-bipyridine) Trichloride: $Rh(bipy)_3Cl_3{\cdot}5H_2O$ Complex. Rhodium trisbipyridine complex was used as an electron mediator. Rhodium trisbipyridine was synthesized according to Kirch et al.[28] Then 30 mL of aqueous ethanol 1:1 (15 mL of H_2O and 15 mL of ethanol) was added to the reaction mixture ((rhodium trichloride (0.55 g; 10.5 mmol), bipyridine (1.2 g; 30.8 mmol) and *N*-ethyl morpholine (2.5 mL)), and the mixture was heated under reflux conditions at 80 °C with frequent shaking. A brown color suspension developed over time. The UV/vis spectrum of the solution was monitored, and the mixture was cooled down as soon as the spectrum showed a peak at ~320 nm and no free bipyridine peak was left at 280 nm. The reaction usually required 30–40 min for completion. Afterward, the reaction mixture was vacuum filtered, and the solvent was pumped off on a rotavapor (Heidolph, HeivAP, Germany). The brownish solid obtained was twice recrystallized from ethanol/water/butanol (50:10:40). The pale yellow crystalline material obtained was washed with the chilled recrystallized solvent mixture and dried under air to yield the complex.

DOI: 10.1021/acs.jpcc.9b10127
J. Phys. Chem. C 2020, 124, 1469–1477

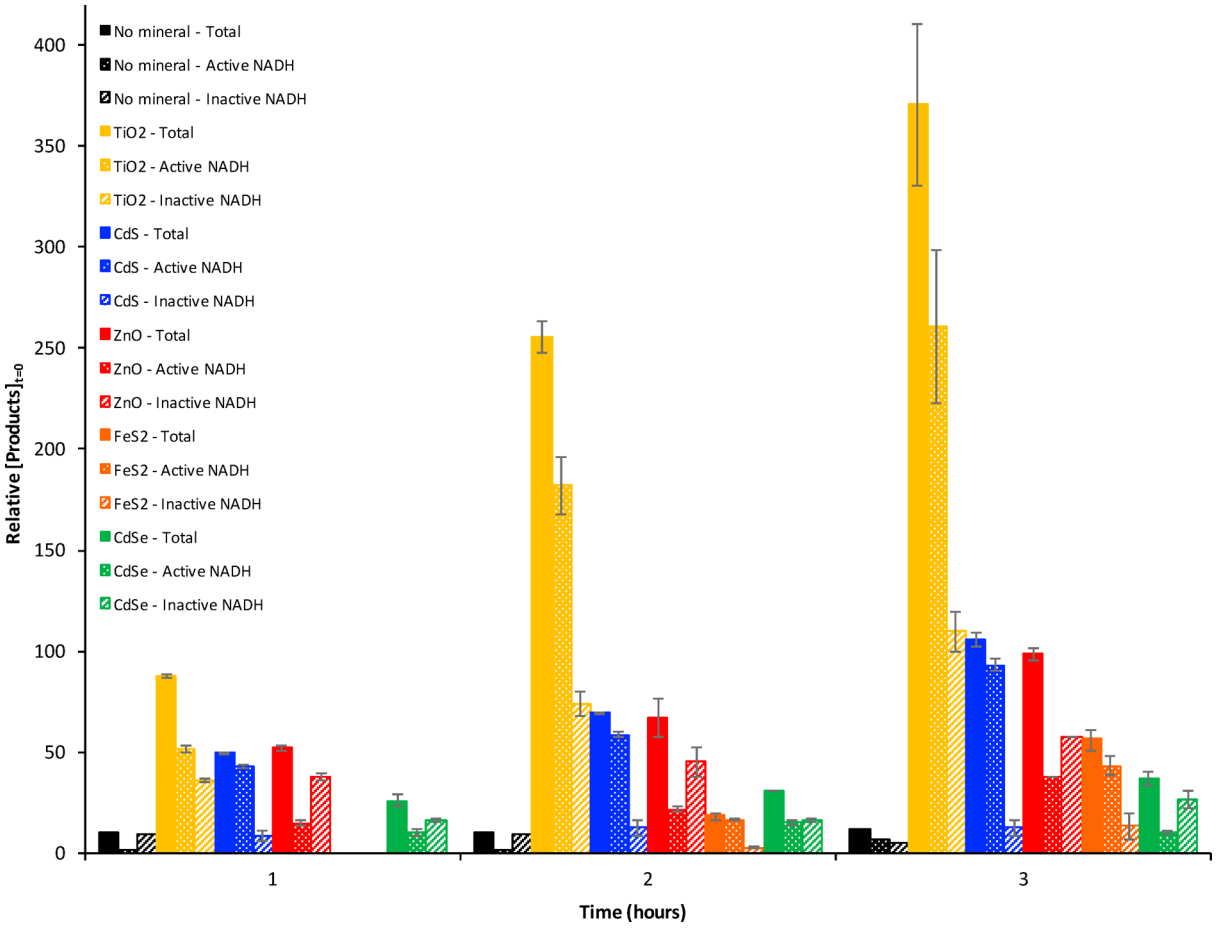

Figure 3. Percentage of TMETR products formed after UV irradiation of 1, 2, and 3 h relative to 0 h in the presence of various photocatalytic minerals. The data from Figure 2 were used to calculate the percent yield of products.

3. RESULTS AND DISCUSSION

3.1. Photocatalytic Minerals Promote TMETR. Nicotinamide adenine dinucleotide can be reduced enzymatically[29] or nonenzymatically in the presence of an electron mediator by electrochemical[30−32] or photochemical[33,34] means. We first investigated the ability of various photocatalytic minerals, CdS, FeS_2, CdSe, TiO_2, ZnO, ZnS, and Cu_2S, to generate NADH from NAD^+ in bulk solutions followed by transmembrane reactions involving vesicles. In bulk solution, the ultraviolet (UV) illumination of these photocatalytic minerals at mildly alkaline pH (8.5) in the presence of NAD^+, $Rh(bipy)_3^{3+}$ complex, and various electron donors led to the formation of NAD products within 1−5 min (Supporting Information, Figures S1 and S2). Photoreduction of NAD^+ produces the enzymatically active and biologically relevant form, 1,4-NADH; the inactive form, 1,6-NADH; and NAD_2 dimers (Scheme S1). All these products have emission spectra near ∼450 nm. Hence, in order to confirm the formation of the active form, the products were reoxidized to NAD^+ using the lactase dehydrogenase (LDH) enzyme (Supporting Information). Biologically active 1,4-NADH was formed in the presence of all minerals except ZnS and Cu_2S. The ZnS and Cu_2S particle sizes are very large, ∼10 and 40 μm, and therefore, they have very low reactive surface area. On the basis of these bulk solution results, we next investigated lipid vesicle systems.

For the TMETR in the model protocell system, terminal electron acceptor (NAD^+) and electron mediator ($Rh(bipy)_3^{3+}$) were encapsulated in POPC vesicles with electron shuttle (naphthopyrene or perylene) embedded in the lipid bilayer. Photocatalytic minerals (CdS, FeS_2, CdSe, TiO_2, and ZnO) and reductant (serine, glycine, or 2-propanol) were added to the extra-vesicular medium (Supporting Information, Methods). We have previously found that vesicles remain intact in the presence of a wide range of minerals,[26] an important feature for the vesicle compartment to be a part of an effective transmembrane reaction. We have found that vesicles were stable up to 3 h of UV radiation (Figure S5). Therefore, the systems were illuminated by UV radiation for up to 3 h. The emission peak at ∼450 nm increases with time indicating progress of the TMETR (Figure 2). A small peak at 383 nm was also observed, ascribed to inelastic scattering.[18]

To confirm formation of active 1,4-NADH, the LDH assay was performed. The NADH peak decreased rapidly after the addition of LDH due to its reconversion to NAD^+, clearly indicating that 1,4-NADH had been produced during the TMETR (Figure 2). The efficiency of producing total NAD products (active NADH, inactive NADH, dimer) decreases according to the sequence TiO_2 > CdS ∼ ZnO > CdSe > FeS_2. In order to separate out the amount of active NADH from the inactive NADH and dimer, the area under the curves from Figure 2 was integrated and is reported in Figure 3 and Table S2. It was found that TiO_2 was the most effective photocatalyst in generating 1,4 NADH followed by CdS, ZnO, FeS_2, and CdSe, respectively. In the case of TiO_2, 4−10 times more TMETR products were formed after 3 h UV irradiation as

DOI: 10.1021/acs.jpcc.9b10127
J. Phys. Chem. C 2020, 124, 1469−1477

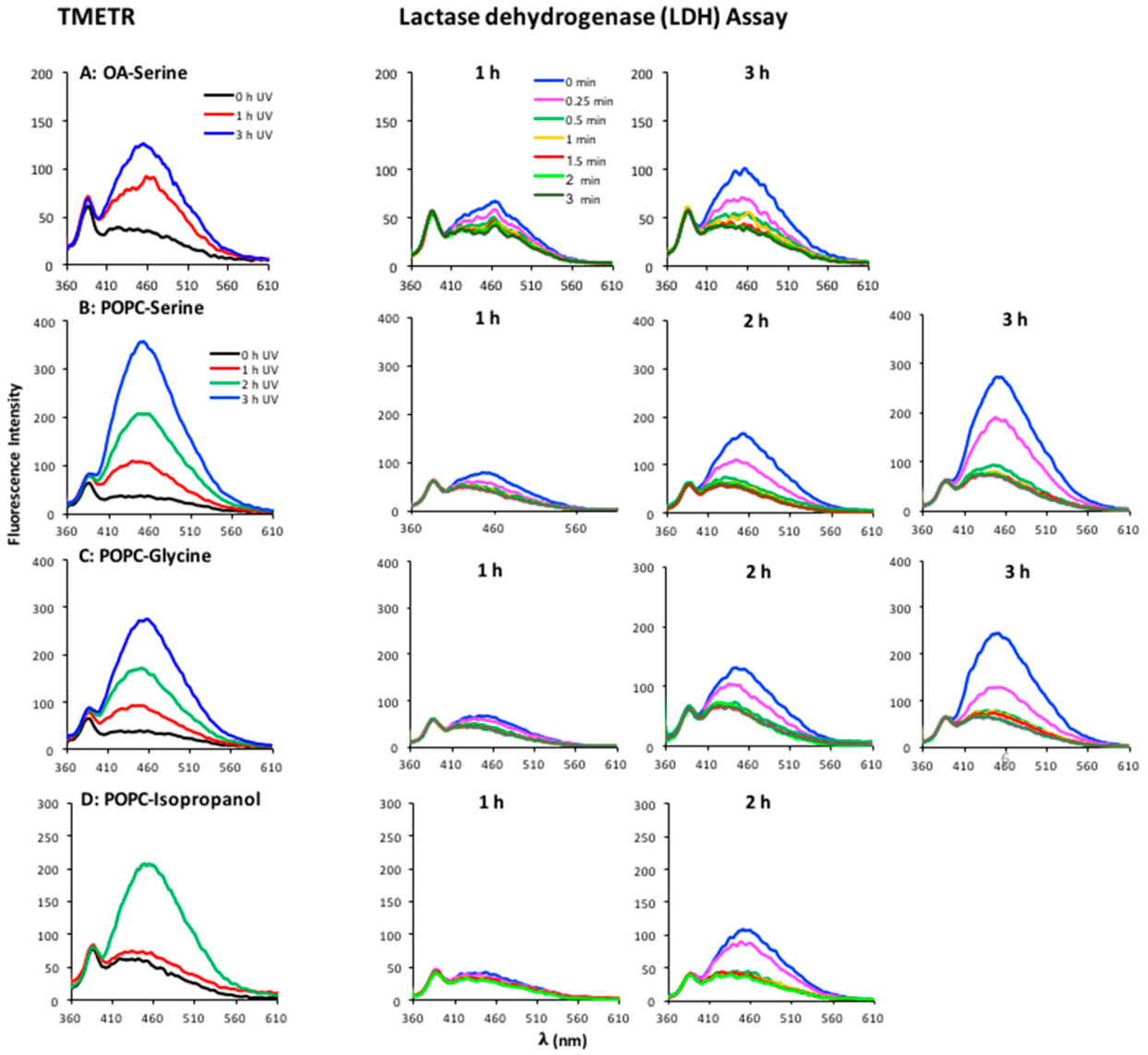

Figure 4. Coupled multistep TMETR photocatalyzed by CdS employing various lipid membranes (A, B) and various terminal electron donors (B–D). (A) Emission spectra of NAD products generated after UV irradiation of OA vesicles encapsulating NAD^+ with extra-vesicular CdS and serine and NP embedded in the bilayer. (B, C, D) Emission spectra of NAD products generated after UV irradiation of POPC vesicles encapsulating NAD^+; extra-vesicular CdS and serine (B) or glycine (C) or 2-propanol (D); and NP embedded in the bilayer. The first graph in each row (left panel) represents the total product formed after 0, 1, 2, and 3 h of UV irradiation and the remaining plots shows the LDH enzyme assay of the TMETR products at each time point (see Supporting Information for details). The legends in the first graphs of both left and right panels are valid for the corresponding panels in the second to fourth rows. Experimental conditions: POPC (2 mM) or OA (7.5 mM), naphthopyrene (50 μM), extravesicular mineral loading (0.5 mg/mL), and electron donor (40 mM), $Rh(bipy)_3^{3+}$ complex (2.5 mM), and NAD^+ (15 mM) in the intravesicular medium. See Supporting Information for details.

compared to other photocatalytic minerals studied after similar duration of irradiation.

In the above-mentioned TMETR's, the photocatalytic activity of minerals was utilized to drive redox cycles inside the vesicles. The hole–electron (h^+–e^-) pair generated by the photocatalytic mineral during the UV-irradiation was separated across the membrane. The terminal electron donor (reductant) added outside the membrane, was oxidized by the holes (h^+) to aldehydes or glyoxylic acid and H^+ along with the generation of NH_3 and CO_2[35−37] (Scheme S2). In the first step of the TMETR process, electrons were transferred from extra-vesicular mineral to the electron shuttle, naphthopyrene, embedded in the bilayer, which subsequently transferred the electron to the intravesicular electron mediator, $Rh(bipy)_3^{3+}$. The $Rh(bipy)_3^{3+}$ was irreversibly reduced to $Rh(bipy)_2^{+}$ by two electrons,[28,33] which were then passed on, as a pair, to NAD^+ to eventually form NADH (Scheme S3). Previous studies of one-step TMETR used methyl viologen or ferricyanide as the electron acceptor from the transmembrane electron transfer because these compounds undergo a colorimetric change which can be tracked by UV–vis absorbance.[16,21] However, neither of these compounds has the ability to transfer two electrons in the next step of the TMETR to NAD^+. Furthermore, NAD_2 formation is suppressed in the presence of $Rh(bipy)_3^{3+}$.[33] Hence, $Rh(bipy)_3^{3+}$ was used in the above TMETR experiments. Importantly, in the absence of $Rh(bipy)_3^{3+}$ complex biologically active 1,4-

DOI: 10.1021/acs.jpcc.9b10127
J. Phys. Chem. C 2020, 124, 1469–1477

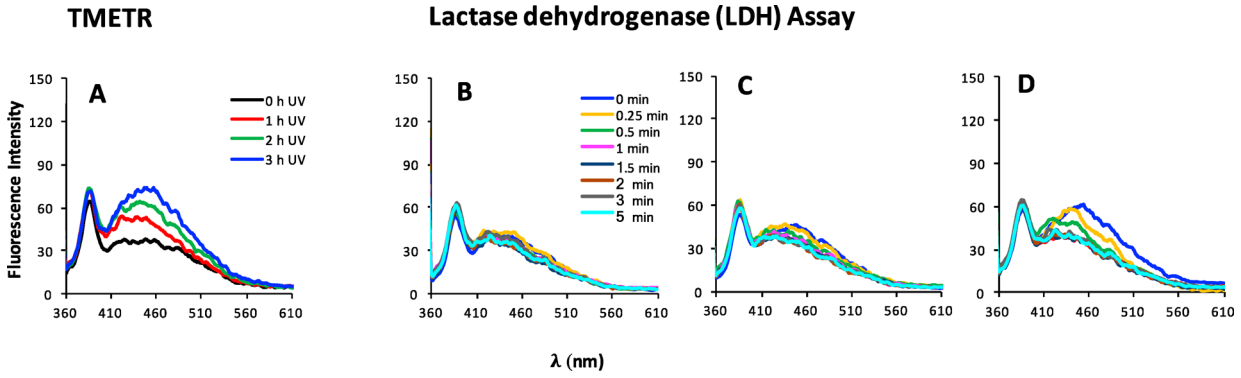

Figure 5. (A) Emission spectra of NAD products generated in the absence of a terminal electron donor after UV irradiation. The system consists of POPC vesicles encapsulating NAD^+ and $Rh(bipy)_3^{3+}$; extravesicular CdS; and NP embedded in the bilayer; (B–D) LDH enzyme assay for the products formed after 1, 2, and 3 h of UV irradiation, respectively. The legend for B is valid for parts C and D. Experimental conditions: POPC (2 mM), naphthopyrene (50 μM), extravesicular mineral loading (0.5 mg/mL), and $Rh(bipy)_3^{3+}$ complex (2.5 mM) and NAD^+ (15 mM) in the intravesicular medium. See Supporting Information for details.

NADH was not formed (Figure S6) and the peak increase was attributed to the inactive NADH and the dimer (Scheme S1).

$Rh(bipy)_3^{3+}$ is used here as a model compound to represent some prebiotic molecule capable of a two-electron transfer. $Rh(bipy)_3^{3+}$ was also used in another protocell experiment where all the reaction components, including oxidant, reductant, electron mediator and photocatalytic mineral, were encapsulated within the vesicle.[18] We can suggest some metal complexes that may be analogues for the rhodium complex, such as metal porphyrins, that can take part in electron transfer reactions. The porphyrin-type metal complexes consist of a macrocyclic tetrapyrrole ligand and a tightly bound metal ion, such as $Fe^{2+/3+}$, Mg^{2+}, Co^{3+}, and Ni^{2+}.[38] Porphyrins and metalated porphyrins could potentially be formed under simulated prebiotic conditions.[39,40]

The effect of particle loading was investigated at 0.5 and 2.0 mg/mL mineral loading. No discernible difference in TMETR was found at higher mineral loading suggesting saturation of available mineral surface (Figure S7, parts A and B).

In the absence of minerals, no reaction products were formed until 1 h UV (Figure S8, parts A and B). The products after 2 and 3 h of UV exposure were found to be enzymatically inactive as indicated by no decrease in the product peak with time in the LDH assay (Figure S8, parts C and D). These results emphasized the essential requirement of photocatalytic minerals to achieve the TMETR.

The minerals used here were chosen were based on their prebiotic availability and their extensive use as semiconductors. For instance, CdS (greenockite) and FeS_2 (pyrite) would have formed under the anoxic conditions on early Earth and FeS_2 has similar structure to the active cores of many photosynthetic enzymes. Titania (rutile and anatase) occurs as an accessory phase in many rocks. CdSe, ZnO (zincite), and TiO_2 are widely used in materials science applications.

3.2. Diverse Protocell Membranes Support TMETR. The above experiments were conducted using POPC, a phospholipid, to form the vesicles. Phospholipids and related lipids have been abiotically synthesized[41−44] and may have been present in mixed lipid membranes in later stages of protocell evolution.[12,13] However, single chain amphiphiles such as fatty acids are generally considered to be more prebiotically plausible compared to pure phospholipid membranes.[45] Therefore, experiments were also conducted with pure oleic acid (OA) vesicles (Figure 4).

The results showed that the TMETR process is not dependent on the type of lipid, as long as the vesicles are impermeable enough to separate intra- and extra-vesicular solutes. However, the emission intensity of NADH in POPC system was higher than for the OA system (Figure 4B versus Figure 4A). This could be due to the presence of a greater number of vesicles in the POPC system as compared to the OA system based on the much lower critical vesicle concentration of POPC. In these experiments, CdS (greenockite) was used for most as it is mineral of a prebiotic relevance. Moreover, CdS was found be an effective prebiotic photocatalyst (Figure 2A and Figure 3).

3.3. PAHs as Electron Shuttle/Electron Wire. Naphthopyrene or perylene were used as the electron shuttle embedded in the membrane (Supporting Information). They were chosen as representative PAH species for their similarities to the PAHs found in chondritic meteorites[45,46] as well as for their favorable photoredox properties. In our TMETR experiments, no discriminable difference was observed between NP and perylene (Figure S7, parts B and C).

Interestingly, when serine is used as a terminal electron donor TMETR was not observed in the absence of PAHs as the electrons cannot pass through the bilayer and neither can serine (Figure S9). As noted earlier, PAHs in the membrane bilayer acts as an electron shuttle for the transfer of electrons. In the absence of electron transfer, NAD^+ was not reduced to NADH and only NAD^+ dimers were formed inside the vesicles (the product peak did not decrease with time in the LDH assay). These results provide evidence that our complete experimental system is a true TMETR without leakage of oxidant or reductant crossing the membrane.

3.4. Simple Organics as Sacrificial Electron Donors. Various simple organic electron donors such serine, glycine, 2-propanol, and methanol were tested in bulk solution (Figure S2) and in vesicle suspensions (Figure 4). The LDH enzyme assay showed the formation of biologically active NADH in the presence of all the reductants (Figure 4). However, note that using methanol as the reductant, the product was formed even in the absence of intramembrane PAH as electron shuttle, demonstrating that methanol is permeable to the membrane (Figure S9B). Hence, the reaction with methanol is not a true TMETR. Interestingly, 2-propanol was impermeable up to 2 h (Figure S9C) unlike methanol, which was found to be permeable soon after adding to the vesicles. Hence, the

DOI: 10.1021/acs.jpcc.9b10127
J. Phys. Chem. C 2020, 124, 1469−1477

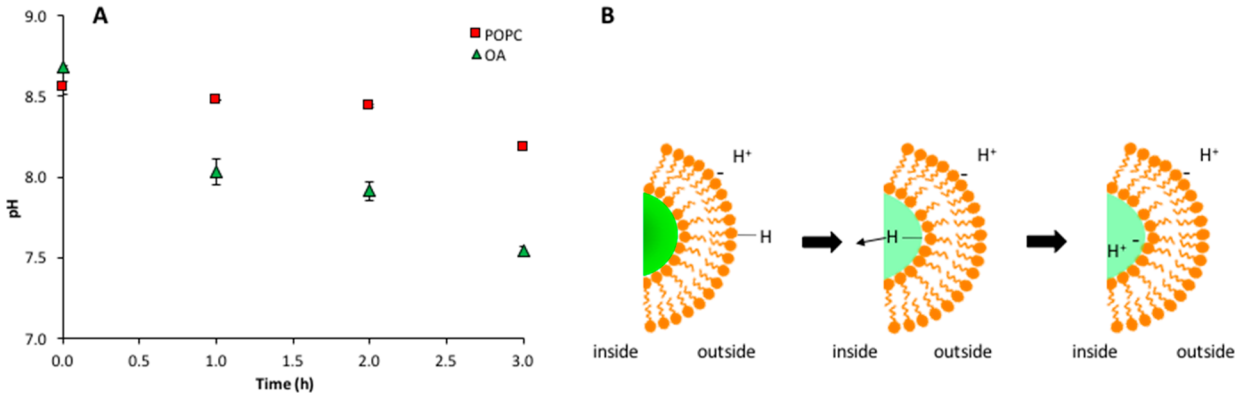

Figure 6. Transmembrane pH gradient generated by the TMETR. (A) Acidification of pure POPC and OA vesicles encapsulated with pyranine dye prepared at pH 8.5. (B) Schematic illustrating the flip-flop mechanism of OA molecules from the outer to the inner leaflet of the membrane with subsequent release of the proton, resulting in acidification of the intravesicular volume.

TMETR using 2-propanol as a reductant was conducted only up to 2 h (Figure 4D).

Photochemical TMETR conversion of NAD^+ to NADH also occurs in vesicles systems lacking any terminal electron donor (Figure 5). However, the amount of 1,4-NADH formed in the absence of electron donor was lower (Figure 5) than in its presence at the same duration of UV irradiation (Figure 4). These results were in agreement with a previous study involving bulk dispersions of TiO_2−NAD^+−$Rh(bipy)_3^{3+}$ complex.[33] In the absence of external sacrificial electron donor, the photocatalytic mineral can act as an electron donor.[47] Meanwhile, the holes generated by UV irradiation can be scavenged by $OH^{\bullet-}$ radicals formed from OH^- groups at the mineral surface.[33]

3.5. Solution pH Affects the TMETR Efficiency. Oceans on the young Earth may have changed from weakly acidic in the early Hadean to near-neutral in the late Hadean eon.[48] Therefore, TMETR experiments were also conducted at pH 7.0 and 7.4 in addition to 8.5 (Figure S10). The enzymatically active form, 1,4-NADH, was only formed at slightly alkaline pH consistent with previous reports that the rate of formation NADH in bulk TiO_2 dispersions increases with increasing solution alkalinity from 7.2 to ∼9.5 and drops at high pHs.[33,34]

In summary, the experiments described above, including those where one component of the TMETR setup is systematically removed to check for the formation of 1,4 NADH, confirm that all the components are required for a TMETR. These experiments also confirm that the present setup represents a true transmemembrane reaction without leakage of oxidant or reductant across the membrane.

3.6. Transmembrane Charge Transfer Generates a Proton Gradient. In the present study, POPC and OA membranes were examined for their potential to develop and maintain a pH gradient across the bilayer. In the TMETR experiments, the oxidation of sacrificial electron donor outside the membrane by the hole generated from the photocatalytic mineral produces protons in addition to aldehydes or glyoxylic acid (Scheme S2). If the protons thus generated cross the bilayer, potentially by lipid "flip-flop" mechanism,[49,50] this would result in a decrease of the intravesicular pH. The pH inside the vesicle is monitored as the change in the fluorescence of encapsulated pyranine, a pH sensitive dye (Figure 6, Supporting Information).

A decrease in fluorescence of pyranine was observed for both types of membranes indicating the acidification of the internal volume. However, in comparison to OA membranes where the pH dropped by 1.2 units, POPC vesicles showed a minimal change in pyranine fluorescence equivalent to ∼0.3 pH units. This result reflects the greater stability and rigidity of the diacyl chains in phospholipids compared to those in single chain amphiphiles. Thus, a pH gradient was generated in the case of both OA and POPC membranes. This gradient was largely maintained across the POPC membrane but was partially dissipated in the case of OA. The magnitude of the transmembrane gradient in the POPC vesicles can be estimated from the pH drop observed across the OA membrane.

Energy transduction through transmembrane proton gradients is an integral part of present day metabolism and may also have been important for the first cells. Several attempts have been made to test the abiotic generation of a pH gradient in liposomes such as by incorporating Fe−S cluster peptide complex in the bilayer,[24] growth of SCA vesicles,[49] loss of cyanide radicals from ferrocyanide by UV illumination[51] and accumulation of charged molecules (amino acids, phosphate, or nucleotides) by convection and thermophoresis.[52] pH gradients have also been generated across pores in iron sulfide precipitates and in a water column by thermophoresis.[22,23,52] The present study provides evidence of a transmembrane pH gradient being generated in lipid vesicles simultaneously with NAD^+ to NADH reduction through a coupled multistep TMETR. The proton gradient generated could have eventually lead to ATP synthesis and the NADH could potentially have been involved in further metabolic reaction.

4. CONCLUSIONS

The origins of life field had largely focused on the prebiotic formation of protocell membranes and RNA with less attention paid to evolution of protometabolism in protocells. The results presented here demonstrate that various photocatalytic minerals present in the extra-vesicular medium can drive redox chemistry inside vesicles by a TMETR resulting in the generation of a proton gradient and simultaneous NADH generation. The present study provides a proof of concept for photocatalytic mineral-promoted transmembrane energy transduction for the emergence of a transitional photoheterotrophic protometabolism in late-stage protocells.

DOI: 10.1021/acs.jpcc.9b10127
J. Phys. Chem. C 2020, 124, 1469−1477

■ ASSOCIATED CONTENT

Supporting Information

The Supporting Information is available free of charge at https://pubs.acs.org/doi/10.1021/acs.jpcc.9b10127.

Materials and methods, Figures S1−S10, Schemes S1−S3, and Tables S1 and S2 (PDF)

■ AUTHOR INFORMATION

Corresponding Author

*(N.S.) E-mail: sahai@uakron.edu.

ORCID

Nita Sahai: 0000-0003-3852-0557

Notes

The authors declare no competing financial interest.

■ ACKNOWLEDGMENTS

N.S. acknowledges financial support provided by the Simons Foundation Origins of Life Initiative award (290359), gift funds from Dr. Ed Weil, and "start-up" funds from the University of Akron. We thank Dr. Steven Mankoci for his help in synthesizing the $Rh(bipy)_3Cl_3$ complex and Dr. Putu Ustriyana for the TEM characterization of the particles. We are grateful for the invaluable conversations with present and former members of the Sahai research group, and with Prof. David Deamer, University of California—Santa Cruz.

■ REFERENCES

(1) Lane, N.; Allen, J. F.; Martin, W. How Did Luca Make a Living? Chemiosmosis in the Origin of Life. *BioEssays* **2010**, *32*, 271−280.

(2) Martin, W.; Russell, M. J. On the Origins of Cells: A Hypothesis for the Evolutionary Transitions from Abiotic Geochemistry to Chemoautotrophic Prokaryotes, and from Prokaryotes to Nucleated Cells. *Philos. Trans. R. Soc., B* **2003**, *358*, 59−85.

(3) Russell, M. J.; Hall, A. The Emergence of Life from Iron Monosulphide Bubbles at a Submarine Hydrothermal Redox and Ph Front. *J. Geol. Soc.* **1997**, *154*, 377−402.

(4) Kim, H. J.; Benner, S. A. A Direct Prebiotic Synthesis of Nicotinamide Nucleotide. *Chem. - Eur. J.* **2018**, *24*, 581−584.

(5) Deamer, D. W.; Oro, J. Role of Lipids in Prebiotic Structures. *BioSystems* **1980**, *12*, 167−175.

(6) Dalai, P.; Sahai, N. Protocell Emergence and Evolution. *Handbook of Astrobiology* **2018**, 491−517.

(7) Adamala, K.; Szostak, J. W. Competition between Model Protocells Driven by an Encapsulated Catalyst. *Nat. Chem.* **2013**, *5*, 495.

(8) Chen, I. A.; Roberts, R. W.; Szostak, J. W. The Emergence of Competition between Model Protocells. *Science* **2004**, *305*, 1474−1476.

(9) Luisi, P. L.; Allegretti, M.; Pereira de Souza, T.; Steiniger, F.; Fahr, A.; Stano, P. Spontaneous Protein Crowding in Liposomes: A New Vista for the Origin of Cellular Metabolism. *ChemBioChem* **2010**, *11*, 1989−1992.

(10) Cheng, Z.; Luisi, P. L. Coexistence and Mutual Competition of Vesicles with Different Size Distributions. *J. Phys. Chem. B* **2003**, *107*, 10940−10945.

(11) Budin, I.; Szostak, J. W. Physical Effects Underlying the Transition from Primitive to Modern Cell Membranes. *Proc. Natl. Acad. Sci. U. S. A.* **2011**, *108*, 5249−5254.

(12) Dalai, P.; Ustriyana, P.; Sahai, N. Aqueous Magnesium as an Environmental Selection Pressure in the Evolution of Phospholipid Membranes on Early Earth. *Geochim. Cosmochim. Acta* **2018**, *223*, 216−228.

(13) Jin, L.; Kamat, N. P.; Jena, S.; Szostak, J. W. Fatty Acid/Phospholipid Blended Membranes: A Potential Intermediate State in Protocellular Evolution. *Small* **2018**, *14*, 1704077.

(14) Lazcano, A.; Miller, S. L. The Origin and Early Evolution of Life: Prebiotic Chemistry, the Pre-Rna World, and Time. *Cell* **1996**, *85*, 793−798.

(15) Ferry, J. G.; House, C. H. The Stepwise Evolution of Early Life Driven by Energy Conservation. *Mol. Biol. Evol.* **2006**, *23*, 1286−1292.

(16) Cape, J. L.; Monnard, P.-A.; Boncella, J. M. Prebiotically Relevant Mixed Fatty Acid Vesicles Support Anionic Solute Encapsulation and Photochemically Catalyzed Trans-Membrane Charge Transport. *Chem. Sci.* **2011**, *2*, 661−671.

(17) Summers, D. P.; Noveron, J.; Basa, R. C. Energy Transduction Inside of Amphiphilic Vesicles: Encapsulation of Photochemically Active Semiconducting Particles. *Origins Life Evol. Biospheres* **2009**, *39*, 127−140.

(18) Summers, D. P.; Rodoni, D. Vesicle Encapsulation of a Nonbiological Photochemical System Capable of Reducing NAD^+ to NADH. *Langmuir* **2015**, *31*, 10633−10637.

(19) Lee, S. H.; Kim, J. H.; Park, C. B. Coupling Photocatalysis and Redox Biocatalysis Toward Biocatalyzed Artificial Photosynthesis. *Chem. - Eur. J.* **2013**, *19*, 4392−4406.

(20) Horvath, O.; Fendler, J. H. Cadmium Sulfide-Particle-Mediated Transmembrane Photoelectron Transfer in Surfactant Vesicles. *J. Phys. Chem.* **1992**, *96*, 9591−9594.

(21) Tunuli, M. S.; Fendler, J. H. Aspects of Artificial Photosynthesis. Photosensitized Electron Transfer across Bilayers, Charge Separation, and Hydrogen Production in Anionic Surfactant Vesicles. *J. Am. Chem. Soc.* **1981**, *103*, 2507−2513.

(22) Barge, L. M.; Kee, T. P.; Doloboff, I. J.; Hampton, J. M.; Ismail, M.; Pourkashanian, M.; Zeytounian, J.; Baum, M. M.; Moss, J. A.; Lin, C.-K. The Fuel Cell Model of Abiogenesis: A New Approach to Origin-of-Life Simulations. *Astrobiology* **2014**, *14*, 254−270.

(23) Möller, F. M.; Kriegel, F.; Kieß, M.; Sojo, V.; Braun, D. Steep pH Gradients and Directed Colloid Transport in a Microfluidic Alkaline Hydrothermal Pore. *Angew. Chem., Int. Ed.* **2017**, *56*, 2340−2344.

(24) Bonfio, C.; Godino, E.; Corsini, M.; de Biani, F. F.; Guella, G.; Mansy, S. S. Prebiotic Iron−Sulfur Peptide Catalysts Generate a pH Gradient across Model Membranes of Late Protocells. *Nat. Catal.* **2018**, *1*, 616.

(25) Cleaves, H. J., II; Scott, A. M.; Hill, F. C.; Leszczynski, J.; Sahai, N.; Hazen, R. Mineral−Organic Interfacial Processes: Potential Roles in the Origins of Life. *Chem. Soc. Rev.* **2012**, *41*, 5502−5525.

(26) Sahai, N.; Kaddour, H.; Dalai, P.; Wang, Z.; Bass, G.; Gao, M. Mineral Surface Chemistry and Nanoparticle-Aggregation Control Membrane Self-Assembly. *Sci. Rep.* **2017**, *7*, 43418.

(27) Kaddour, H.; Gerislioglu, S.; Dalai, P.; Miyoshi, T.; Wesdemiotis, C.; Sahai, N. Non-Enzymatic RNA Oligomerization at the Mineral-Water Interface: An Insight into the Adsorption-Polymerization Relationship. *J. Phys. Chem. C* **2018**, *122*, 29386−29397.

(28) Kirch, M.; Lehn, J. M.; Sauvage, J. P. Hydrogen Generation by Visible Light Irradiation of Aqueous Solutions of Metal Complexes. An Approach to the Photochemical Conversion and Storage of Solar Energy. *Helv. Chim. Acta* **1979**, *62*, 1345−1384.

(29) Abril, O.; Whitesides, G. M. Hybrid Organometallic/Enzymic Catalyst Systems: Regeneration of NADH Using Dihydrogen. *J. Am. Chem. Soc.* **1982**, *104*, 1552−1554.

(30) Jaegfeldt, H. A Study of the Products Formed in the Electrochemical Reduction of Nicotinamide-Adenine-Dinucleotide. *J. Electroanal. Chem. Interfacial Electrochem.* **1981**, *128*, 355−370.

(31) Schmakel, C. O.; Santhanam, K.; Elving, P. J. Nicotinamide Adenine Dinucleotide (NAD^+) and Related Compounds. Electrochemical Redox Pattern and Allied Chemical Behavior. *J. Am. Chem. Soc.* **1975**, *97*, 5083−5092.

(32) Wienkamp, R.; Steckhan, E. Indirect Electrochemical Regeneration of NADH by a Bipyridinerhodium (I) Complex as Electron-Transfer Agent. *Angew. Chem., Int. Ed. Engl.* **1982**, *21*, 782−783.

DOI: 10.1021/acs.jpcc.9b10127
J. Phys. Chem. C 2020, 124, 1469−1477

(33) Cuendet, P.; Graetzel, M. Photoreduction of NAD to NADH in Semiconductor Dispersions. *Photochem. Photobiol.* **1984**, *39*, 609−612.
(34) Bojarska, E.; Pawlicki, K.; Czochralska, B. Photocatalytic Reduction of Nicotinamide Coenzymes in the Presence of Titanium Dioxide: The Influence of Aliphatic Aminoacids. *J. Photochem. Photobiol., A* **1997**, *108*, 207−213.
(35) Overend, R.; Paraskevopoulos, G. Rates of Hydroxyl Radical Reactions. 4. Reactions with Methanol, Ethanol, 1-Propanol, and 2-Propanol at 296 K. *J. Phys. Chem.* **1978**, *82*, 1329−1333.
(36) Pascual, R.; Herráez, M. A. The Mechanism of the Oxidative Deamination and Decarboxylation of Serine and Threonine by Periodate in Acid Medium. *Can. J. Chem.* **1985**, *63*, 2349−2353.
(37) Shi, H.; Shen, S.; Sun, H.; Liu, Z.; Li, L. Oxidation of L-Serine and L-Threonine by Bis (Hydrogen Periodato) Argentate (Iii) Complex Anion: A Mechanistic Study. *J. Inorg. Biochem.* **2007**, *101*, 165−172.
(38) Kaim, W.; Schwederski, B.; Klein, A. *Bioinorganic Chemistry-Inorganic Elements in the Chemistry of Life: An Introduction and Guide*; John Wiley & Sons, 2013; pp 22−31, 37−116, 172−177.
(39) Fox, S.; Strasdeit, H. A Possible Prebiotic Origin on Volcanic Islands of Oligopyrrole-Type Photopigments and Electron Transfer Cofactors. *Astrobiology* **2013**, *13*, 578−595.
(40) Pleyer, H. L.; Strasdeit, H.; Fox, S. A Possible Prebiotic Ancestry of Porphyrin-Type Protein Cofactors. *Origins Life Evol. Biospheres* **2018**, *48*, 347−371.
(41) Hargreaves, W.; Mulvihill, S.; Deamer, D. Synthesis of Phospholipids and Membranes in Prebiotic Conditions. *Nature* **1977**, *266*, 78.
(42) Rao, M.; Eichberg, J.; Oró, J. Synthesis of Phosphatidylcholine under Possible Primitive Earth Conditions. *J. Mol. Evol.* **1982**, *18*, 196−202.
(43) Maheen, G.; Tian, G.; Wang, Y.; He, C.; Shi, Z.; Yuan, H.; Feng, S. Resolving the Enigma of Prebiotic C-O-P Bond Formation: Prebiotic Hydrothermal Synthesis of Important Biological Phosphate Esters. *Heteroat. Chem.* **2010**, *21*, 161−167.
(44) Patel, B. H.; Percivalle, C.; Ritson, D. J.; Duffy, C. D.; Sutherland, J. D. Common Origins of RNA, Protein and Lipid Precursors in a Cyanosulfidic Protometabolism. *Nat. Chem.* **2015**, *7*, 301−307.
(45) Dalai, P.; Kaddour, H.; Sahai, N. Incubating Life: Prebiotic Sources of Organics for the Origin of Life. *Elements* **2016**, *12*, 401−406.
(46) Sephton, M. A. Organic Compounds in Carbonaceous Meteorites. *Nat. Prod. Rep.* **2002**, *19*, 292−311.
(47) Moser, J.; Graetzel, M. Light-Induced Electron Transfer in Colloidal Semiconductor Dispersions: Single Vs. Dielectronic Reduction of Acceptors by Conduction-Band Electrons. *J. Am. Chem. Soc.* **1983**, *105*, 6547−6555.
(48) Morse, J. W.; Mackenzie, F. T. Hadean Ocean Carbonate Geochemistry. *Aquat. Geochem.* **1998**, *4*, 301−319.
(49) Chen, I. A.; Szostak, J. W. Membrane Growth Can Generate a Transmembrane pH Gradient in Fatty Acid Vesicles. *Proc. Natl. Acad. Sci. U. S. A.* **2004**, *101*, 7965−7970.
(50) Kamp, F.; Hamilton, J. A. pH Gradients across Phospholipid Membranes Caused by Fast Flip-Flop of Un-Ionized Fatty Acids. *Proc. Natl. Acad. Sci. U. S. A.* **1992**, *89*, 11367−11370.
(51) Deamer, D.; Harang, E. Light-Dependent pH Gradients Are Generated in Liposomes Containing Ferrocyanide. *BioSystems* **1990**, *24*, 1−4.
(52) Keil, L. M.; Möller, F. M.; Kieß, M.; Kudella, P. W.; Mast, C. B. Proton Gradients and pH Oscillations Emerge from Heat Flow at the Microscale. *Nat. Commun.* **2017**, *8*, 1897.

DOI: 10.1021/acs.jpcc.9b10127
J. Phys. Chem. C 2020, 124, 1469−1477